This full text paper was peer reviewed at the direction of IEEE Communications Society subject matter experts for publication in the IEEE ICC 2010 proceedings

Influences of Vehicles on Signal Propagation in Road Tunnels

Zhi Sun and **Ian F. Akyildiz**
Broadband Wireless Networking Laboratory (BWN Lab)
School of Electrical & Computer Engineering, Georgia Institute of Technology, Atlanta, GA, 30332, USA
Email: {zsun; ian}@ece.gatech.edu

***Abstract*—It is well known that the electromagnetic (EM) waves do not propagate well in road tunnels. The channel characteristics for empty tunnels have already been well analyzed by both theoretical and numerical/experimental methods. However, any road tunnels are full with running vehicles. Currently a few works have investigated the influence of the vehicles on the signal propagation in road tunnels. However, they are all limited to experimental or numerical results. This paper provides a theoretical mode-based analysis to give the straightforward description of the wireless channel in road tunnels with traffic flow. First the effects of a single vehicle in the tunnel are investigated. The analytical expressions of the *in-mode loss* and the *mode coupling* are provided using uniform theory of diffraction (UTD), Poisson summation formula and saddle point method. Then the channel model for a L-lane road tunnel with the Poisson traffic flow is provided basing on the analysis on single vehicle's effect.**

I. Introduction

Electromagnetic (EM) waves do not propagate well in tunnels. Due to the reflections on tunnel walls, the multipath fading in these environments is much more severe than the terrestrial wireless channels [1]. Moreover, the operating road tunnels are filled with mobile vehicles with random size and positions. The reflections and diffractions on the vehicles make the wireless channel in tunnels even more complicated. To setup reliable and efficient wireless communication systems in road tunnels, we need the analytical channel model that explicitly contains the dependence on the tunnel geometry, traffic information, and other communication parameters.

For empty tunnels, currently there are mainly three techniques to model the wireless channel: the Geometrical Optical model (GO model) [2], the Waveguide model [3] and the Full Wave model [4]. The GO model and the Full Wave model are limited to numerical results and may create great computational burden. The waveguide model provides analytical results but is only applicable for the far region of the transmitter in empty tunnels. In [1], we have developed the Multipath model that gives analytical results for both the near region and the far region in an empty tunnel. However the model cannot characterize the influence of vehicles in the tunnel. For tunnels with vehicles, current solutions are based on either experiments [6] or numerical methods (GO model [7], [8] and Full Wave model [9]). However, the experimental and numerical solutions cannot provide explicit description on the effect of tunnel geometry, the traffic information, antenna position/polarization, operating frequency, and other environment or communication parameters. Currently there is no analytical channel model presented to characterize the signal propagation in road tunnels with traffics.

In this paper, we develop the channel model to analytically characterize the signal propagation in road tunnels with traffic flows. In particular, we implement the Multimode model to calculate the signal propagation in the empty part of the road tunnel. Around a vehicle in the tunnel, each propagation mode is converted to four plane waves with different directions. Due to the reflections and the diffractions of the plain waves on the vehicle, it may incur *in-mode loss* and *mode coupling* of each propagation mode. The closed-form of the in-mode loss and mode coupling coefficients is developed by uniform theory of diffraction (UTD) [10], Poisson sum formula [11] and saddle point method. The field at the receiver is the joint effects of all the vehicles between the transceivers and the tunnel itself. Besides deterministic scenario, the statistical model for random traffic flows is also presented by considering the traffic flow as a Poisson process. Our analytical model is validated by comparing the theoretical predictions with the numerical results. Based on the new channel model, we present an in-depth analysis on the signal propagation in tunnels with traffic, which is influenced by multiple factors including the number, size and position of the vehicles, the size and the curvature of the tunnel, the traffic load, and the vehicle velocity.

The remainder of this paper is organized as follows. In Section II, the Multimode model for empty tunnels is overviewed. In Section III, the signal propagation around a single vehicle is analyzed. In Section IV, the channel model for road tunnels with multiple vehicles are developed. Then, in Section V, the influence of the vehicles on signal propagation is analyzed by the new model. Finally, the paper is concluded in Section VI.

II. Signal Propagation in Empty Tunnels

In this section, the Multimode model for empty tunnels [1] is briefly overviewed, which lays the foundation of the analysis on the signal propagation in tunnels with vehicles. Specifically, the empty tunnel is modeled as an oversized waveguide with imperfectly lossy walls. Multiple waveguide modes with different eigenfunctions and attenuation coefficients are transmitting simultaneously in the tunnel. The tunnel cross section is treated as an equivalent rectangular with a width of $2a$ m and a height of $2b$ m. A Cartesian coordinate system is set with its origin located at the center of the

† This work was supported by the US National Science Foundation (NSF) under Grant No. CCF-0728889.

978-1-4244-6404-3/10/$26.00 ©2010 IEEE

rectangle tunnel. The electric field $E^{RX}(x,y,z)$ at the position of the receiver can be obtained by summing up the field of all propagation modes, which is given by:

$$E^{RX}(x,y,z) = \frac{\sqrt{G_t G_r}}{2k} \sum_N E^{eign}_{N,(x,y)} \cdot \exp(-\Gamma_N \cdot z) \cdot C^{Tx}_N \quad (1)$$

where z is the distance between the transmitter and the receiver; (x,y) is the coordinate of the receiver at the tunnel cross section; G_t and G_r are the TX and RX antenna gain, respectively; k is the wave number; $E^{eign}_{N,(x,y)}$ is the value of the N^{th} mode's eigenfunction at the receiver's position; Γ_N is the attenuation coefficient of the N^{th} mode; C^{Tx}_N is the N^{th} mode's intensity induced by the transmitter. The detailed expression of $E^{eign}_{N,(x,y)}$ and Γ_N can be found in [1], [5]. C^{Tx}_N is calculated by projecting the EM field excited by the transmitter on the eigenfunction of the N_{th} mode:

$$C^{Tx}_N = \int_{-a}^{a}\int_{-b}^{b} E^{Tx}_{(x,\ y)} \cdot E^{eign}_{N,(x,\ y)}\ dx\, dy \quad (2)$$

where $E^{Tx}_{(x,\ y)}$ is the EM field excited by the TX antenna at the position (x,y) on the excitation plane, which is calculated by the Geometrical Optical (GO) model.

III. Signal Propagation around a Single Vehicle

The propagation modes can travel along the tunnel without interference with each other if the tunnel is empty. Vehicles in the tunnel may cause additional propagation loss of each mode, which is regarded as *in-mode loss*. Moreover, part of the energy of each mode may be coupled to the other modes due to the existence of the vehicles, which is regarded as *mode coupling*. In this section, we analyze the influence of a single vehicle on the mode propagation inside the tunnel.

Without loss of generality, the vehicles are modeled as metal cubes with different sizes. According to US Federal Regulations, the width w, height h and length l of most vehicles (including cars, vans, buses and trucks) fall into the following intervals (unit is meter):

$$w \in [1.5, 2.5], \quad h \in [1.3, 4.2], \quad l \in [3.5, 16.2] \quad (3)$$

A. Classification of Vehicle Influence

We assume that the TX antenna is a X-polarized electrical dipole (horizontal polarization) in the deduction of this section. The results for Y-polarized antenna can be obtained in the similar way. The tunnel walls are made of concrete that have relative permittivity ε_w. The wave number in the tunnel space is given by $k = 2\pi f\sqrt{\mu_0 \varepsilon_0}$, where μ_0 and ε_0 are the permeability and the permittivity of the air in the tunnel, respectively; and f is the operating frequency. Since the permittivity ε_w of the concrete tunnel wall is much larger than 1 and the wave number k is also large for high operating frequency (> 1 GHz), the eigenfunction of X-polarized mode EH_{mn} provided by [1] can be simplified as:

$$E^{eign}_{mn,(x,\ y)} \simeq \sin\left(\frac{m\pi}{2a}x + \varphi_x\right) \cdot \cos\left(\frac{n\pi}{2b}y + \varphi_y\right) \quad (4)$$

where $\varphi_x = 0$ if m is even; $\varphi_x = \frac{\pi}{2}$ if m is odd; $\varphi_y = 0$ if n is odd; $\varphi_y = \frac{\pi}{2}$ if n is even.

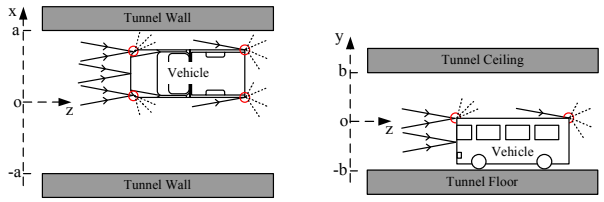

(a) Top view (b) Side view

Fig. 1. In-mode loss due to the reflection on the front surface. Mode coupling due to the diffraction on the two horizontal edges and four vertical edges.

Assuming that there is a vehicle with size $(w \times h \times l)$ inside the tunnel. Fig. 1 shows the top view and the side view of the tunnel with a vehicle. The vehicle is z_v meters apart from the transmitter. The middle axle of the vehicle lies parallel to the z-axes with the position $x = x_v$. In the empty tunnel between the transmitter and the vehicle, the field of EH_{mn} mode is:

$$\begin{aligned} E_{mn}(x,y,z) &= C^{Tx}_{mn} \cdot e^{-\Gamma_{mn} \cdot z} \cdot E^{eign}_{mn,(x,y)} \\ &= \frac{1}{4} C^{Tx}_{mn} \cdot \big\{ \rho_1(m)\rho_2(n) e^{ik[x\sin(\alpha_m) + y\sin(\beta_n) - \Gamma_{mn}/k \cdot z]} \\ &\quad + \rho_2(m)\rho_2(n) e^{ik[x\sin(-\alpha_m) + y\sin(\beta_n) - \Gamma_{mn}/k \cdot z]} \\ &\quad + \rho_1(m)\rho_1(n) e^{ik[x\sin(\alpha_m) + y\sin(-\beta_n) - \Gamma_{mn}/k \cdot z]} \\ &\quad + \rho_2(m)\rho_1(n) e^{ik[x\sin(-\alpha_m) + y\sin(-\beta_n) - \Gamma_{mn}/k \cdot z]} \big\} \end{aligned} \quad (5)$$

where $\rho_1(u) = -j$ if u is even; $\rho_1(u) = 1$ if u is odd; $\rho_2(u) = j$ if u is even; $\rho_2(u) = 1$ if u is odd. It shows that each propagation mode can be viewed as the superposition of four plane waves with four symmetric directions. $\pm\alpha_m$ and $\pm\beta_n$ are the grazing angles of the plane waves on the tunnel walls, which satisfy:

$$\sin(\alpha_m) = \frac{m\pi}{2ak}; \quad \sin(\beta_n) = \frac{n\pi}{2bk} \quad (6)$$

It indicates that the higher order modes have larger grazing angles. Since higher order mode has much higher attenuation rate [1], we pay more attention on the lower order modes. For the lowest order mode EH_{11}, the grazing angle is very small.

As illustrated in Fig. 1, the vehicle can affect the propagation mode in two ways:

- The plane waves hitting the vehicle's front surface will be reflected back. The energy reflected back can be viewed as additional loss of the EH_{mn} mode caused by the vehicle. This kind of influence is defined as *in-mode loss*.
- The plane waves hitting the edge between two surfaces of the vehicle will be diffracted. The diffracted waves has different transmission directions, which means that the energy is coupled to other modes. This kind of influence is defined as *mode coupling*.

B. In-Mode Loss

The in-mode loss is first calculated. The eigenfunction of the propagation mode gives the energy distribution pattern in the tunnel cross section of each mode. Basing on the eigenfunctions, the energy reflected back by the vehicle's front

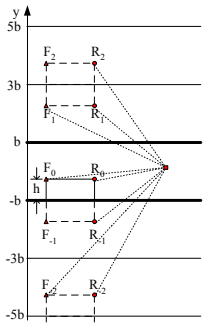

Fig. 2. Side view (y-z plane) of the diffractions on the horizontal edges of a vehicle in the tunnel.

surface can be obtained. The in-mode loss is the ratio of the energy reflected back to the total energy in the cross section:

$$L_{mn} = \frac{\int_{x_v-\frac{w}{2}}^{x_v+\frac{w}{2}}\int_{-b}^{-b+h}[E^{eign}_{mn,(x,y)}]^2dxdy}{\int_{-a}^{a}\int_{-b}^{b}[E^{eign}_{mn,(x,y)}]^2dxdy} \tag{7}$$
$$= \frac{1}{4ab}\Big[w - \frac{2a}{m\pi}(-1)^m\cos(\frac{m\pi}{a}x_v)\sin(\frac{m\pi}{a}w)\Big] \cdot \Big[h - \frac{b}{n\pi}\sin(\frac{n\pi}{b}h)\Big]$$

It shows that the in-mode loss is a function of the width, height and the position of the vehicle. Actually, in the interval of the tunnel where the vehicle exists, the mode attenuation coefficient Γ_{mn} increases. It is because that the tunnel cross section in this interval is smaller than the empty tunnel. The increased attenuation coefficient causes the additional in-mode loss. However, this part of in-mode loss can be ignored for low order modes, which is due to the reason that the attenuation coefficient is small for low order mode and the vehicle length is relatively short (less than 20 m).

C. Mode Coupling

The diffraction on the vehicle edges causes a portion of one mode's energy coupling to other modes. According to Fig. 1, the diffraction occurs on the four vertical edges and the two horizontal edges on the vehicle. Using the geometrical theory of diffraction (GTD) [12], we can proof that the vertical edge on an obstruction can only cause one mode to be coupled to the modes that have the same eigenfunctions on y-axes (the eigenfunctions on x-axes can be different). In other words, when mode EH_{mn} is diffracted on a vertical edge, it can only be coupled to the modes $\{EH_{tn}|t=1,2,\cdots\}$. Similarly, when mode EH_{mn} is diffracted on a horizontal edge, it can only be coupled to the modes $\{EH_{ms}|s=1,2,\cdots\}$. Then the mode coupling analysis in tunnels can be simplified to two 2-dimensional problems: the mode coupling in x-z plane for the four vertical edges; and the mode coupling in y-z plane for the two horizontal edges.

Fig. 2 shows the diffracted rays on the two horizontal edges in the y-z plane. The propagation mode EH_{mn} hits the front upper horizontal edge F_0 and the rear upper horizontal edge R_0. Since the attenuation coefficient of the low order mode is small and the vehicle length is usually several meters, the field attenuation and phase shift from the vehicle front to the rear can be ignored. Hence the fields at the front edge can be considered as the same as the field at the rear edge, which is:

$$E^i_{mn} = C^{Tx}_{mn}\cdot e^{-\Gamma_{mn}\cdot z_v}\cdot E^{eign}_{mn,(x,h-b)} \tag{8}$$
$$= C^{Tx}_{mn}\cdot e^{-\Gamma_{mn}\cdot z_v}\cdot\sin\Big(\frac{m\pi}{2a}x+\varphi_x\Big) \cdot\frac{1}{2}\Big[\rho_2(n)e^{ik(h-b)\sin(\beta_n)}+\rho_1(n)e^{ik(h-b)\sin(-\beta_n)}\Big]$$
$$\triangleq E^i_{mn}(\beta_n)+E^i_{mn}(-\beta_n)$$

where we view the field as the sum of two rays with grazing angle $\pm\beta_n$ on y-z plane.

1) Mode Coupling on the Rear Horizontal Edge: We first consider the diffracted field caused by the rear edge. Note that only the incident rays with direction $-\beta_n$ is considered for the diffractions on the rear edge, which is due to the reason that rays with direction β_n cannot hit the rear edge, as shown in Fig. 1(b). The edge can be viewed as a new radiation source. Due to the reflections on the tunnel ceiling/floor, the new source generates periodically positioned source images, as shown in Fig. 2. The diffracted field caused by the rear edge can be calculated by summing up all the rays coming from all the images, which is:

$$E^D(x,y,z+z_v) \tag{9}$$
$$= \sum_{p=-\infty}^{\infty}E^i_{mn}(-\beta_n)\cdot D(\alpha_m,\pi\mp\phi_p,\beta_n)\cdot R(\phi_p)^{|p|}\cdot\frac{e^{-jkr_p}}{\sqrt{r_p}}$$

where the upper sign is used for the case when p is zero, positive odd or negative even; the lower sign is for other cases; r_p is the distance from image R_p in Fig. 2; ϕ_p is the angle of the grazing angle on the tunnel celing/floor of the rays coming from image R_p; it is also the diffracted angle on the y-z plane. $R(\phi_p)$ is the reflection coefficient that can be simplified as an exponential function [1]. $D(\theta_1,\theta_2,\theta_3)$ is the diffraction coefficient on an edge, where $\frac{\pi}{2}-\theta_1$ is the angle between the incident ray and the edge; θ_2 is the angle of the diffracted ray on the plane perpendicular to the edge; and θ_3 is the angle of the incident ray on the plane perpendicular to the edge. Since the GTD method cannot characterize the diffraction near the shadow boundary and the reflection boundary, we adopt unified theory of diffraction (UTD) to calculate the coefficients, which is given in [10, fomula (25)].

To calculate the energy coupled to the other modes, the Poisson summation formula [11] is introduced to translate the sum of rays in (9) to the sum of modes. Therefore the total field right behind the vehicle ($z\simeq 0$) can be expressed as:

$$E^D(x,y,0+z_v) \tag{10}$$
$$= \frac{1}{4b}E^i_{mn}(-\beta_n)\sum_{s=1}^{\infty}\big[D(\alpha_m,\pi-\beta_s,\beta_n)+D(\alpha_m,\pi+\beta_s,\beta_n)\big] \cdot\frac{\sqrt{2\pi k}}{k\cos(\beta_s)}\cdot\cos\Big(\frac{s\pi}{2b}h+\varphi_y\Big)\cdot\cos\Big(\frac{s\pi}{2b}y+\varphi_y\Big)$$

Note that the second line in (10) is exact the sum of the propagation modes. The total contribution caused by the whole edge

can be calculated by integrate (10) along the horizontal edge. Therefore we can derive the coupling coefficient $B^{r,h}_{mn\to ms}$ from EH_{mn} to EH_{ms} caused by the rear horizontal edge:

$$B^{r,h}_{mn\to ms} = \sin(\frac{m\pi x_v}{2a}+\varphi_x)\sin(\frac{m\pi w}{4a})\cdot\cos(\frac{s\pi}{2b}h+\varphi_y) \cdot\big[D(\alpha_m,\pi-\beta_s,\beta_n)+D(\alpha_m,\pi+\beta_s,\beta_n)\big] \cdot\frac{a\sqrt{2\pi k}}{2m\pi kb\cos(\beta_s)}\cdot\rho_1(n)\cdot e^{ik(h-b)\sin(-\beta_n)} \quad (11)$$

2) Mode Coupling on the Front Horizontal Edge: The mode coupling coefficient for the front horizontal edge can be calculated in the similar way as the rear horizontal edge. As shown in Fig. 2, the only two differences are: 1) the incident waves have both the directions $\pm\beta_n$; and 2) due to the shadow effect of the vehicle itself, not all the images can illuminate the rest of the tunnel; Only the original source, the images with positive odd subscripts and the images with negative subscripts take effects. As a result, the coupling coefficient $B^{f,h}_{mn\to ms}$ from EH_{mn} to EH_{ms} caused by the front horizontal edge can be expressed as:

$$B^{f,h}_{mn\to ms} = \sin(\frac{m\pi x_v}{2a}+\varphi_x)\sin(\frac{m\pi w}{4a})\cdot\cos(\frac{s\pi}{2b}h+\varphi_y) \cdot\frac{a\sqrt{2\pi k}}{2m\pi kb\cos(\beta_s)}\cdot\Big\{\rho_1(n)\cdot e^{ik(h-b)\sin(-\beta_n)}\cdot D(\alpha_m,\pi-\beta_s,\beta_n) +\rho_2(n)\cdot e^{ik(h-b)\sin(\beta_n)}\cdot D(\alpha_m,\pi-\beta_s,-\beta_n)\Big\} \quad (12)$$

3) Total Mode Coupling: The mode coupling coefficient for the four vertical edges can be derived in the same way as the horizontal edges. We only need to interchange the x-axes data and the y-axes data. Therefore the total coupling coefficient $B^{total}_{mn\to ms}$ from EH_{mn} to EH_{ms} caused by the vehicle is the sum of the coefficients of the two horizontal edges:

$$B^{total}_{mn\to ms}=\sin(\frac{m\pi x_v}{2a}+\varphi_x)\sin(\frac{m\pi w}{4a})\cdot\cos(\frac{s\pi}{2b}h+\varphi_y) \quad (13)$$
$$\cdot\frac{a\sqrt{2\pi k}}{2m\pi kb\cos(\beta_s)}\cdot\Big\{\rho_2(n)\cdot e^{ik(h-b)\sin(\beta_n)}\cdot D(\alpha_m,\pi-\beta_s,-\beta_n) +\rho_1(n)\cdot e^{ik(h-b)\sin(-\beta_n)}\cdot\big[2D(\alpha_m,\pi-\beta_s,\beta_n)+D(\alpha_m,\pi+\beta_s,\beta_n)\big]\Big\}$$

The total coupling coefficient $B^{total}_{mn\to tn}$ from EH_{mn} to EH_{tn} caused by the vehicle is the sum of the coefficients of the four vertical edges:

$$B^{total}_{mn\to tn}=(-1)^{\lceil\frac{n}{2}\rceil}\cdot\frac{b\sqrt{2\pi k}}{2n\pi ka\cos(\alpha_t)}\cdot\cos(\frac{n\pi}{2b}h) \quad (14)$$
$$\cdot\Big\{\cos\big(\frac{t\pi}{2a}(x_v+\frac{w}{2})\big)\cdot\Big[\rho_1(m)e^{ik(x_v+\frac{w}{2})\sin(\alpha_m)}\cdot D(\beta_n,\pi-\alpha_t,-\alpha_m) +\rho_2(m)e^{ik(x_v+\frac{w}{2})\sin(-\alpha_m)}\cdot\Big(2D(\beta_n,\pi-\alpha_t,\alpha_m)+D(\beta_n,\pi+\alpha_t,\alpha_m)\Big)\Big]$$
$$+\cos\big(\frac{t\pi}{2a}(x_v-\frac{w}{2})\big)\cdot\Big[\rho_2(m)e^{ik(x_v-\frac{w}{2})\sin(-\alpha_m)}\cdot D(\beta_n,\pi+\alpha_t,\alpha_m) +\rho_1(m)e^{ik(x_v-\frac{w}{2})\sin(\alpha_m)}\cdot\Big(2D(\beta_n,\pi+\alpha_t,-\alpha_m)+D(\beta_n,\pi-\alpha_t,-\alpha_m)\Big)\Big]\Big\}$$

D. Analytical Expression of a Single Vehicle's Effect

We construct the influence matrix of a vehicle using the results shown in (7), (13) and (14). If there are $\overline{N}$ significant modes inside the tunnel, the size of the influence matrix $\mathbf{I}$ is $\overline{N}\times\overline{N}$. The elements in the diagonal of the matrix consist of the in-mode loss of each significant mode, which is given by (7). The other elements in the matrix are the mode coupling coefficients. Note that mode coupling can only happen between two modes that has the same field distribution either in x-z plane or y-z plane. The coupling coefficients between those modes are given by (13) and (14). The mode coupling coefficients between other modes are zero. Given the size and the position of the vehicle, its influence on the signal propagation can be analytically expressed by using the influence matrix. Hence, the intensity of all the significant modes behind a vehicle inside the tunnel are:

$$\begin{pmatrix}C'_1\\C'_2\\\vdots\\C'_{\overline{N}}\end{pmatrix}=\begin{pmatrix}1-L_1 & B^{total}_{2\to1} & \cdots & B^{total}_{\overline{N}\to1}\\ B^{total}_{1\to2} & 1-L_2 & \cdots & B^{total}_{\overline{N}\to2}\\ \vdots & \vdots & \ddots & \vdots\\ B^{total}_{1\to\overline{N}} & B^{total}_{2\to\overline{N}} & \cdots & 1-L_{\overline{N}}\end{pmatrix}\cdot\begin{pmatrix}C_1\\C_2\\\vdots\\C_{\overline{N}}\end{pmatrix} \quad (15)$$

where $\{C_1,C_2,\ldots,C_{\overline{N}}\}$ are the intensity of all the significant modes before the vehicle; and $\{C'_1,C'_2,\ldots,C'_{\overline{N}}\}$ are the intensity behind the vehicle.

IV. Channel Model for L-Lane Road Tunnels

In this section, the channel model for a L-lane ($L=1,2,\ldots$) road tunnel with traffic is provided. We first develop the deterministic model for the case when the geometric information of both the tunnel and the vehicles are known. The predicted received power is compared with the numerical result provided in [7]. Then we present the statistical model for the case when the tunnel geometric information is given but the number, sizes and the positions of the vehicles are not known.

A. Deterministic Model

Assuming that there are M vehicles between the transceivers in the tunnel. The tunnel geometry is the same as the previous section. The position and size of the i^{th} vehicle are (x^i_v,z^i_v) and (w_i,h_i,l_i), respectively. The transmitter is placed in the tunnel cross section where $z=z_0$ and the receiver is placed at (x_r,y_r,z_r). The field intensity at the position of the receiver can be expressed as:

$$E^{RX}(x_r,y_r,z_r)=\mathbf{E}^{eign}_{(x_r,y_r)}\cdot\mathbf{A}(z_r-z_M)\cdot\prod_{i=1}^{M}\Big[\mathbf{I}_i\cdot\mathbf{A}(z_i-z_{i-1})\Big]\cdot\mathbf{C}^{TX} \quad (16)$$

where $\mathbf{E}^{eign}_{(x_r,y_r)}$ is the eigenfunction vector at (x_r,y_r):

$$\mathbf{E}^{eign}_{(x_r,y_r)}=\Big[E^{eign}_{1,(x_r,y_r)},E^{eign}_{2,(x_r,y_r)},\cdots E^{eign}_{\overline{N},(x_r,y_r)}\Big] \quad (17)$$

$\mathbf{A}(z)$ is the $\overline{N}\times\overline{N}$ mode attenuation matrix for transmitting all the significant modes for z meters in an empty tunnel. It is a diagonal matrix where the i^{th} element on the matrix diagonal is $e^{-\Gamma_i\cdot z}$ while other elements not in the diagonal are zero. $\mathbf{I}_i$ is the influence matrix caused by the i^{th} vehicle that is defined in (15). $\mathbf{C}^{TX}$ is the mode intensity vector excited by the transmitter at z_0: $\mathbf{C}^{TX}=\big[C^{TX}_1,C^{TX}_2,\cdots C^{TX}_{\overline{N}}\big]^T$.

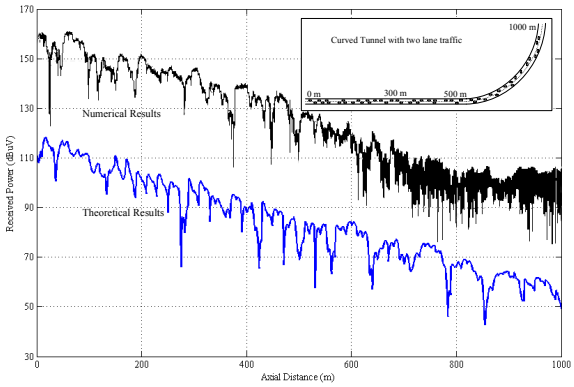

Fig. 3. Numerical and theoretical received power in a curved tunnel with traffic (the numerical one is displaced 40 dBuV upward for better comparison).

B. Comparison with Numerical Results

Since it is difficult to conduct experiments in the operating road tunnel with running vehicles, we validate our theoretical model with the numerical results provided in [7]. The numerical results gives the received power in a two-lane curved road tunnel under the influence of 48 cars and trucks. The tunnel geometry and the vehicle positions are briefly shown in Fig. 3. Using the same parameters, the received power is calculated by our determined model as shown in Fig. 3. The theoretical curve is compared with the numerical results given in [7, Bild 6.7]. It is shown that the two curves have a good match.

C. Statistical Model

In practical applications, the exact sizes and positions of all the vehicles in the tunnel cannot be acquired. Instead of using the deterministic traffic information, we adopt the traffic flow theory and the vehicle size distribution model to predict the signal propagation inside an operating road tunnel. In long road tunnels, there is usually no traffic lights and the traffic flow has only one direction (separate tunnels for traffic with different directions). In addition, we assume that the traffic load is not high and the average vehicle running velocity is v. Hence the traffic flow can be modeled as a Poisson flow [13]. The total number of the vehicles within the distance d is denoted as M. The probability of $M = m$ is:

$$P(m) = \left(\lambda \frac{d}{v}\right)^m \cdot \frac{1}{m!} \cdot e^{-\lambda \frac{d}{v}} \tag{18}$$

where λ is the average rate of vehicle arrival (vehicles/sec) in the road tunnel. The distance between the i^{th} and $(i-1)^{th}$ vehicle $(z_i - z_{i-1})$ obeys independent exponential distribution. The probability density function (pdf) is:

$$f(z_i - z_{i-1}) = \lambda \cdot e^{-\lambda \frac{z_i - z_{i-1}}{v}} \tag{19}$$

Every vehicle runs in one of the L lanes in the tunnel. Hence the x-coordinate of the i^{th} vehicles x_v^i belongs to $\{a(\frac{1+2l}{L} - 1) | l = 0, 1, \ldots L-1\}$. The x-coordinate of the vehicle obeys uniform distribution with the probability $1/L$. The size of the vehicles are also assumed to have the uniform distribution in the size interval defined in (3). In the statistical model, although the received power is still calculated by (16), it should be noted that the vehicle number M, vehicle position (x_v^i, z_v^i) and vehicle size (w_i, h_i, l_i) are random variables that are defined in the above discussion.

V. Analysis on Vehicle's Influence

In this section, we first use the deterministic model to analyze the effects of the size, number and the positions of the vehicles in both a straight one-lane tunnel and a straight two-lane tunnel. Then, the statistical model is utilized to give the received power as a function of the transmission distance, traffic load and vehicle average velocity, in both a straight two-lane tunnel and a curved two-lane tunnel.

The environment and communication parameters are set as follows: the tunnel cross section shape is a rectangle with the size of $10\ m \times 6\ m$ for two-lane tunnels and the size of $6\ m \times 5\ m$ for one-lane tunnels. The transmitting and receiving antennas are vertically polarized dipoles at the same height (one-third of the tunnel height). Both antennas are placed at the same horizontal position of one-quarter of the tunnel width. The transmitting antenna has the power of 1 W and the impedance of 50 Ω. The operating frequency is 1 GHz.

A. Tunnels with Deterministic Vehicles

1) One-Lane Road Tunnel: Fig. 4(a) illustrates the effects of vehicles' size, number and position on the received power in a straight one-lane. The existence of the vehicles causes the two effects: the additional channel loss caused by the in-mode loss and additional signal fluctuation caused by the mode coupling. Comparing the received power when there are 10 trucks inside the tunnel and the power when there are 20 trucks, we find that the additional loss and fluctuation are approximately proportional to the number of vehicles. The size of the vehicle has significant effects on the path loss, since the influence of 10 cars is much smaller than the influence of the 10 trucks. We compare the received power when 10 truck are uniformly placed in the 1 km tunnel and the case when all the trucks are placed in the first 500 m of the tunnel. It indicates that the influence of the vehicles' position is not significant.

2) Two-Lane Road Tunnel: Fig 4(b) shows that the signal propagation in a two-lane road tunnel, where the path loss and signal fluctuation are much smaller than the one-lane tunnel. The effect of vehicles on the signal propagation is not as significant as the one-lane tunnel case, which can be explained by the following reasons: 1) the two-lane tunnel has a larger cross section. Hence the signal attenuation of each mode in the empty tunnel is smaller than the one-lane case. 2) the ratio of the vehicle's cross section area to the tunnel's cross section area is much smaller than the one-lane case, hence the in-mode loss and the mode coupling become less significant.

B. Tunnels with Random Vehicles

In this part, the traffic load is described using the average rate of vehicle arrival λ. We define $\lambda = 0.2$ as the high traffic load case and $\lambda = 0.05$ as the low traffic load case. In the same way, we denote the average vehicle velocity $v = 72$ km/h as the high speed case and $v = 36$ km/h as the high speed case.

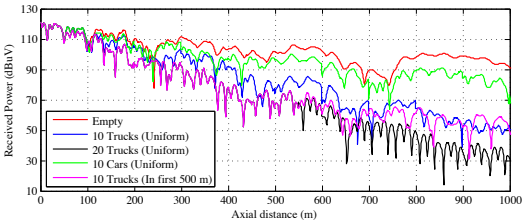

(a) Received signal power in straight one-lane road tunnel.

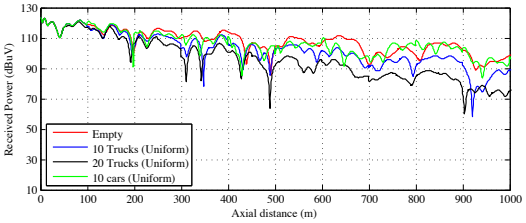

(b) Received signal power in straight two-lane road tunnel.

Fig. 4. Influence of determined vehicles in straight 1-lane/2-lane road tunnels.

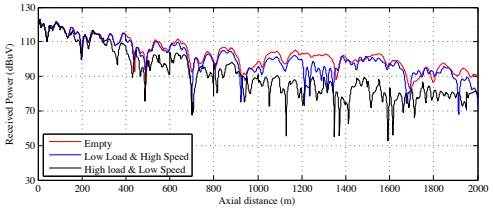

(a) Received signal power in straight two-lane road tunnel.

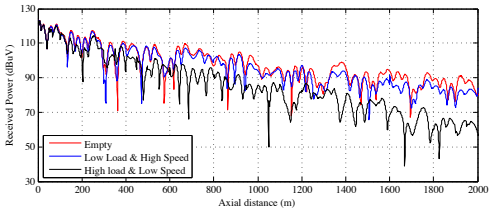

(b) Received signal power in curved two-lane road tunnel.

Fig. 5. Influence of random vehicles in straight/curved 2-lane road tunnels.

1) Straight Tunnel: Fig. 5(a) shows the received power under the influence of two types of traffic flows in a straight tunnel. The received power is shown as a function of the transmission distance. The influence of the traffic flow with lower load and higher speed is less significant than the higher load and lower speed case. When the traffic load is light, fewer vehicles enter the tunnel. When the average vehicle speed is high, the vehicles in the tunnel leave the tunnel more quickly. Consequently, the number of vehicles in the tunnel is smaller. According to the previous discussion on the effects of vehicle number, the effect of the traffic flow should be less significant.

2) Curved Tunnel: Fig. 5(b) illustrates the signal propagations in a curved tunnel with two types of traffic flows. The curve radius of the tunnel is 1 km. The influence of the vehicles on the signal propagation is similar to the straight tunnel case. When the traffic is light and the average speed is high, the signal fluctuation is more severe than the straight tunnel case. It should be noted that this additional fluctuation is not caused by the vehicles but the tunnel curvature.

VI. Conclusion

In this paper, we provide a closed-form expression that can accurately predict the signal propagation and field distribution in any position of a road tunnel with traffics. Specifically, the Multimodel model is used in the tunnel where there is no vehicle. The propagation modes experience in-mode loss and mode coupling around a vehicle. The UTD method, Poisson sum formula and saddle point method are utilized to calculate the in-mode loss and mode coupling coefficients. Besides the deterministic model, a statistical model that takes the traffic flow model into consideration is also presented. Based on the proposed channel model, our analysis shows that: the vehicles in road tunnels will cause additional path loss and signal fluctuations. In the deterministic case when all the information of the vehicles are known, the number and size of the vehicle, as well as the size of the tunnel determine the intensity of the vehicles' influence. In the case when the geometry information of the vehicles are not known, the average vehicle arriving rate and the average vehicle velocity determine the additional loss and signal fluctuation caused by the vehicles.

References

[1] Z. Sun and I. F. Akyildiz, "Channel Modeling of Wireless Networks in Tunnels," in *Proc. IEEE GLOBECOM 2008*, New Orleans, USA, November 2008.

[2] Y. Hwang, Y. P. Zhang and R. G. Kouyoumjian, "Ray-Optical Prediction of Radio-Wave Propagation Characteristics in Tunnel Environments Part 1: Theory, Part 2: Analysis and Measurements" *IEEE Trans. on Antenna and Propagation*, vol. 46, no. 9, pp. 1328-1345, September 1998.

[3] A. G. Emslie, R. L. Lagace and P. F. Strong, "Theory of the Propagation of UHF Radio Waves in Coal Mine Tunnels," *IEEE Trans. on Antenna and Propagation*, vol. AP-23, no. 2, pp. 192-205, March 1975.

[4] A. Taflove and S. C. Hagness, *Computational Electrodynamics: The Finite-Difference Time-Domain Method*, 3rd ed. Norwood, MA: Artech House, 2005.

[5] A. V. Popov and N. Y. Zhu, "Modeling Radio Wave Propagation in Tunnels with a Vectorial Parabolic Equation," *IEEE Trans. on Antenna and Propagation*, vol. 48, no. 9, pp. 1403-1412, September 2000.

[6] Y. Yamaguchi, T. Abe and T. Sekiguchi, "Radio wave propagation loss in the VHF to microwave region due tovehicles in tunnels," *IEEE Trans. on Electromagnetic Compatibility*, vol. 31, no. 1, pp. 87-91, February 1989.

[7] AWE Communications, "Entwicklung eines Programmpakets fur die Berechnung der Ausbreitung elektromagnetischer Wellen in Tunnels," *Technical Report*, http://www.awe-communications.com/Propagation/Tunnel/pdf/tunnel.pdf

[8] S.H. Chen and S.K. Jeng, "BR image approach for radio wave propagation in tunnels with andwithout traffic" *IEEE Trans. on Vehicular Technology*, vol. 45, no. 3, pp. 570-578, August 1996.

[9] K. Arshad, F.A. Katsriku and A. Lasebae, "Modelling obstructions in straight and curved rectangular tunnels by finite element approach," *Journal of Electrical Engineering* , vol. 59, no. 1, pp. 9-13, 2008.

[10] R.G. Kouyoumjian and P.H. Pathak, "A uniform geometrical theory of diffraction for an edge in a perfectly conducting surface," *Proceedings of the IEEE*, vol. 62, No.11, pp. 1448-1461, November 1974.

[11] H. Y. Yee, L. B. Felsen, and J. B. Keller, "Ray theory of reflection from the open end of awaveguide," *SIAM J. Appl. Math.*, vol. 16, No.2, pp. 268300, March 1968.

[12] V.A. Borovikov and B. Ye. Kinber, *Geometrical theory of diffraction*, London: Institution of Electrical Engineers, 1994.

[13] D. L. Gerlough and M. J. Huber, *Traffic Flow Theory: A Monograph*, Washington: Transportation Research Board, National Research Council, 1975.